COMPUTATIONAL AND MATHEMATICAL ANALYSIS OF DYNAMICS OF FUSED DEPOSITION MODELLING BASED RAPID PROTOTYPING TECHNIQUE FOR SCAFFOLD FABRICATION

A Thesis submitted in partial fulfilment of the requirements for the degree of

Master of Technology

In

Biomedical Engineering

By

ALANKAR AGRAWAL

212BM1348

Under The Supervision of

Prof. (Mrs.) Krishna Pramanik

Department of Biotechnology & Medical Engineering
National Institute of Technology
Rourkela-769008, Orissa, India
June, 2014

National Institute of Technology

Rourkela

CERTIFICATE

This is to certify that the thesis entitled, "***COMPUTATIONAL AND MATHEMATICAL ANALYSIS OF THE DYNAMICS OF FUSED DEPOSITION MODELLING BASED RAPID PROTOTYPING TECHNIQUE FOR SCAFFOLD FABRICATION***" submitted by **Alankar Agrawal (212BM1348)** in partial fulfillment of the requirements for the award of degree of **Master of Technology** in **Biomedical Engineering** at National Institute of Technology, Rourkela is an authentic work carried out by him under my supervision and guidance. To the best of my knowledge, the matter embodied in the thesis has not been submitted to any other University/Institute for the award of any Degree or Diploma.

Place: Rourkela

Date:

Supervisor

Prof. Krishna. Pramanik

Department of Biotechnology and Medical Engineering

National Institute of Technology, Rourkela-769008

ABSTRACT

Fused Deposition Modelling (FDM) based rapid prototying technique, is basically used to fabricate three dimensional (3D) objects. Recently, the technique has been considered as the most promising for fabrication of 3D scaffold from polymeric materials for biomedical application including tissue engineering. It is further reported that the scaffold designed from FDM by layer by layer deposition process does not mimic geometry as designed in the computer aided design (CAD) software. In this context, the adjustment of instrument parameters such as extruder nozzle diameter, nozzle angle and liquefier length is of paramount importance to achieve improved extruded melt flow behaviour and scaffold design. Therefore, this main focus of this thesis work is to analyse the flow behaviour of PCL scaffold material using computational and mathematical tools by varying extruded nozzle diameter, nozzle angle and nozzle length of the existing FDM machine. This analysis shows that the reduction in nozzle diameter and nozzle angle, results in higher pressure drops that leading to fine geometry of the scaffold.

The proposed designed suggests that the nozzle diameter can be decreased from 0.5mm to 0.2mm with a nozzle angle of 120 degrees, that will increase the pressure at the nozzle tip and decrease extruded melt diameter that contributes better resolution during scaffold fabrication.

Key Words: Fused Deposition Modelling, 3D scaffold, Polycaprolactone , thermoplastic , CAD.

ACKNOWLEDGEMENT

It is my pleasure to take the opportunity of expressing my sincere gratitude to all those people who provided their support, collaboration and encouragement to carry out my dissertation work. This project helped me a lot to extract out practical knowledge from theoretical work.

First of all I would like to thank my supervisor, ***Prof. Krishna Pramanik,*** *HOD, Department of Biotechnology and Medical Engineering, NIT Rourkela, for her invaluable guidance and help in my dissertation work. I also thank her for guiding me during every part of my work, for helping me improve upon my mistakes all through the project workand for her kind cooperation, inspiration and providing experimental expertise required in my work.*

I would like to extend my thanks to ***Dr. S. K, Sarangi****, Director, National Institute of Technology, Rourkela for providing the opportunity and facilities to pursue this work at the institute.*

I have an overwhelming sense of gratitude to Mr. Niladri Panda, Mr. Aklabya Bissoyi, Mr. Nadeem Siddiqui, Ms. Varshini Vishwanath, Mr. B. N .Singh, Mr. Partha Sartha Majhi and Ms. Parinita Agrawal for imparting knowledge on various topics of my field of research and actively concerned about experimental analysis. I have learnt many experimental techniques from them. I appreciate the skills and art they have, to make others understand any problem.

I am also thankful to entire technical and non-teaching staff of Department of Biotechnology and Medical Engineering, NIT Rourkela for their co-operation and help in completing my dissertation work.

Finally, I would like to express my sincere gratitude to my parents Mr . K. D. Agarwal and Mrs. Uma Agarwal. I am extremely grateful to my sister Ms. Prerana Agarwal and brother Rajat Agarwal for believing, inspiring and supporting me at every step of my life.

Alankar Agrawal

CONTENTS

List of Figures

List of Tables

Nomenclature

Symbols	**Defination**
h_1, h_2 *and* h_3	Height of geometric sections of the liquefier
α	Nozzle Angle
I.F	Integrating Factor.
$\emptyset$	Fluidity Constant
m	Melt Flow Index
v	Input / Entrance Velocity
T	Temperature slightly above the PCL melting temperature
T_a	Absolute temperature
T_0	Temperatute at which $\emptyset$ and m are calculated
D	Inlet diameter of the nozzle
d	Existing diameter of the nozzle / filament diameter at nozzle exit
r	radius
η	Viscosity
E_a	Activation Energy
T_d	Torqueproducedin motor
R_s	Radius of the motor shaft
F	Force
ω	Angular Velocity
R	Radius of the circular section of the nozzle
r_i	Inserting radius of the nozzle

r_e	exiting radius of the nozzle
τ	Shear Stress
$\dot{v}$	Average velocity of the fluid flow in the three sections of the nozzle.
Δp	Pressure Drop

CHAPTER 1 : INTRODUCTION AND OBJECTIVE

1.1 Introduction

Fused deposition modeling (FDM) has become a broadly used rapid prototyping technology. FDM process has variety of applications in numeous fields such as mechanical engineering, biomedical engineering and tissue engineering etc. In tissue engineering, a highly porous artificial extracellular matrix refer to as scaffold is required for the cells proliferation, cell migration, growth and formation of three-dimension (3D) tissue. However, conventional technique for fabrication of 3D scaffolds for tissue engineering is not ideal for real medical applications because they have less mechanical strength, interconnected pores, and controlled porosity or pores distribution. So, the use of RP process is considered as a prominent technique for the fabrication of tissue engineering scaffold [1].

In FDM, utilized in this study (Makerbot Thing –o- matic model) a filament of plastic material is supplied on a roll and fed into a liquefier which is connected with a heater, where it is melted. This melted form of material is then extruded by a nozzle while the feeded filament, remains in it's original phase. The nozzle is mounted to a mechanical point which might be moved in the *xy* plane. As the nozzle is moved over the platform in a prespecified geometry, it deposits a thin droplet of plastic material extruded from the extruder, which solidifies quickly when come in contact with substrate. Solid layers are created by following a rastering movement where the droplets are deposited side by side inside an obtrusive boundary . Successful bonding of the droplets in the deposition process is the fundamental parameter for the control of thermal enviorment. Therfore, the entire system is encased inside a chamber, which is kept up at a temperature marginally lower than the melting point of the material being deposited. When a first layer is completed, the platform is brought down in the z direction so as to begin the next layer. This methodology proceeds until the creation of the fabrication of object is completed is finished [2].

Several materials are commonly used for this process including polymers such as Polycaprolactone (PCl), Polylacticacid (PLA) etc. The scaffold prepared from FDM have some irregularities in its geometry and orientation due to melt flow behaviour of the material or some other parameters of the machine component. Pressure drop, nozzle exit diameter and nozzle angle are the key parameters responsible for these irregularities. The modification in these parameters provides the scaffold of better resolution, orientation and fine geometry [3].

Earlier, Bellini studied some parameters such as, deposition speed and flow rate of the FDM technique to improve the design of the scaffold using theoretical and neumerical concept. The result showed a major difference between the theoretical and neumerical analysis [2]. In this thesis, the correlation of pressure drop with nozzle angle and nozzle diameter was studied. The analysis was performed using two method, first by mathematical modeling and other via CFD modeling. The pressure drop at varying nozzle diameter and nozzle angle was calculated using both the analysis and it's effect on the fabrication of scaffold was then studied.

1.2 Objective

The specific objective of the project is as follows-

1. To improve the design of the liquefier of FDM technique
2. To study CFD analysis of the dynamics of FDM technique
3. To study mathematical analysis of the dynamics of FDM technique
4. To study different parameters of the improved design of liquefier for proper fabrication of the scaffold
5. To compare CFD and Mathematical analysis

CHAPTER 2 : LITERATURE REVIEW

2.1 Rapid Prototyping (RP)

Rapid prototyping is a process of fabrication where the materials are added layer by layer to specific points in space to construct a solid object. This type of technology is also called layered manufacturing, rapid manufacturing or additive fabrication technique. At initial stage of this technology was mainly used to build smaller models or prototypes of new products or products being developed, but due to their much wider range of applications, they are now being used in different fields such as mechanical engineering, biomedical engineering etc. This technology can be used in various fields depending upon their need and quality desired. Rapid prototyping involves a process in which a 3D model of the desired object is built layer by layer through the process of additive fabrication[3].

There are various types of RP process available today. It can be classified based on the intial form of its material. It can be categorized as ***(i) liquid – based, (ii) powder – based, and (iii) solid-based.***

2.1.1 Liquid-based RP method

Liquid-based RP systems have intial form of their material in liquid form. Through a methodology ordinarily known as curing, the liquid is converted into solid state.

2.1.1.1 Stereolithography (SLA)

Stereolithography is one of the most established RP procedure, created by Charles W. Body in the year 1986 [4]. This was later commercialized by 3D systems Inc. economically in the year 1987. **Lee et. al.** desribes the working standard of stereolithography. SLA uses a noticeable or perhaps ultraviolet laser beam and deciphering procedure in order to harden selectively water photocurable resin and design any level that has a cross-sectional appearance that was earlier geared up coming from laptop or computer assisted pattern (CAD) info from the product to get made. Through rehashing the particular structuring cellular levels in a chosen course, the particular craved three-dimensional shape is designed level by level. This action hardens the particular try to sell in order to 96 % regarding full hardening. In the awaken to construct, the

particular designed aspect will be place that has a ultraviolet oven to get treated approximately 100 %, and i. e. any postcuring method [5]. The points of interest of stereolithography are that (1) it indicates the best precision of construct parts (2) prototypes made by SLA might be exceptionally helpful as they are solid enough to be machined and can be utilized as examples for infusion embellishment, thermoforming, blow forming, and additionally in different metal throwing procedures [6]. The disadvantages are that, the material utilized as a part of SLA is exceptionally costly and harmful, The process has a restricted choices of material.(3) The part can be weakened which might have an effect on the surface as soon as evacuated [6].

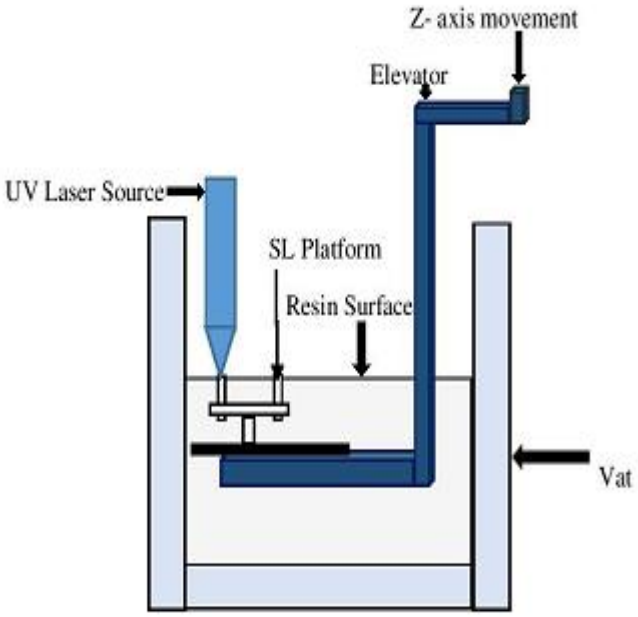

Figure 2.1 : Working model of Stereolithography (SLA) process

2.1.2Powder-based RP method

Powder based RP technique uses material in powder form to construct 3D model. The use of the powder as the constructive medium facilitates the 3D printing to utilize the extensive variety of materials such as metals, polymeric substances, ceramics, etc [7].

The advantages of powder based rapid prototyping process includes, it can handle wide range of processing materials with no post-processing and post-curing required.The disadvantages are that large physical size of the unit, high power consumption and poor surface finish [8].

2.1.2.1 Selective Laser Sintering (SLS)

Selective Laser Sintering (SLS) RP technique was designed by the University of Texas and commercialized by DTM in the year 1987. It uses materials in fine powders formto developed the model. The powder is fused together by a beam of carbon dioxide ($CO_{2)}$ laser.

The methodology starts with the warming of whole power couch, keeping in mind the end goal to minimize warm contortion and facilitate to the past layer. While using assemble cylindrical tube on top, a slim coating involving powder is actually distribute in the manufacture region by a roller/sweeper through on the list of food cylinders. The particular workstation-controlled laser beam draws required device-way, in this way produces a single coating by healing your powdered. The particular cyndrical tube is actually as compared to less complicated and much more powdered is actually maintained. The task is actually rehashed right up until if your portion is completed. At the moment, portion is actually shifted to the Break Out station (BOS) where the additional powdered is actually uprooted together with brushes [9].

The benefits of this method are (1) the extensive variety of fabricate materials, (2) higher throughput capability. Whereas the detriments are (1) higher starting up and maintenance cost, (2) the requirement regarding peripherals, for instance, BOS table, oxygen handler and sifter (to channel the dirt particles from the zone) [10].

2.1.2.2 Laser Engineered Net Shaping (LENS)

The LENS technique, produced by Sandia National Laboratories along with popularized by means of Optomec Style Corp. with 1997, is really a RP strategy suit in making absolutely thicker metal or cermet areas by means of intertwining powders into the core sector of a laser shaft. Similar to almost all RP techniques, LENS also ties an additional material making technique [11]. The high-fueled beam of the laser is usually based onto some sort of substrate where by metal powdered ingredients is usually infused underneath appliance path. Every time a stratum is usually produced, the point is usually made possible location decrease to setup the procedure for the next stratum.

As the center of the laser moves, quick hardening happens making a completely thick material. The majority of this happens inside a construct chamber that keeps up a dormant environment. Moreover, powder that is not devoured by a layer may be recouped and utilized once more. Because of the fast hardening predominant quality and flexibility are accomplished [12].

The advantages of the LENS procedure is that it looks at the sourcing of a completely heavy portion created from the powdered of a individual stuff without further warm healing; this is incredible in the field of RP [13]. Additionally, it includes the capacity to apply transforming sytheses connected with powdered (i.ethe steel contaminants blended thoroughly having ceramic particles) henceforth making it possible for people for making cermets, multi-metal. Henceforth, it is possible to process a portion with shifting materials and characteristics in order to satisfy the prerequisites of a particular provision , for example , die cast tooling .

2.1.2.3 3D Printer

In the 3D inkjet printer technology , produced by MIT and after that commercialized by Z Corporation in the year 1994 , layers of powders are linked to a substrate and consequently merged on implementing a fastener splashed via a spout. The part is inherent the layer by layer

fashion, immediately after each layer, the cylinder is brought down and new powder is included. In the wake of buiding the element, the overabundance powder, that was supporting the model is evacuated. With a specific end goal to uproot the powder caught inside the product, element require to incorporate a gap [14].

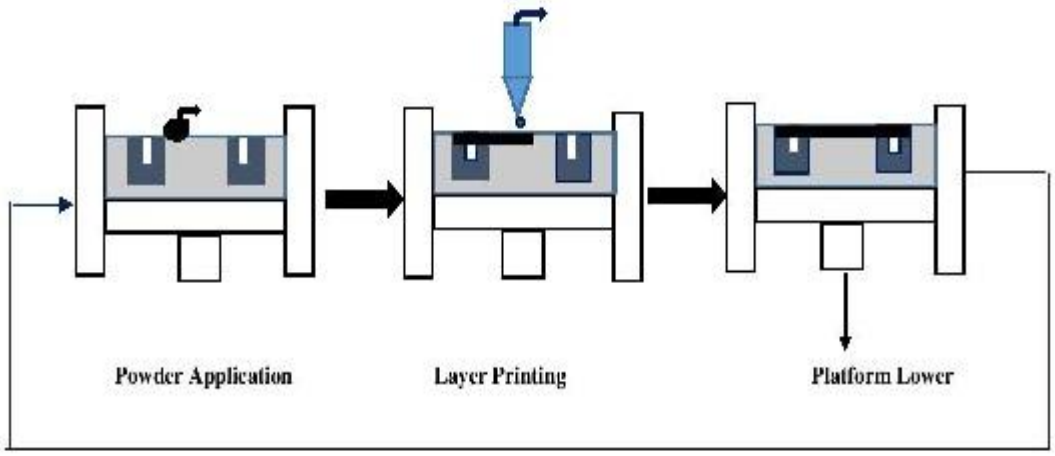

The cycle is repetitive

Figure 2.2 : Schematic diagram of 3D Printing process

2.1.3 Solid-based RP method

Those procedures which utilize solid based materials, bond together solid sheets with a laser or with a adhesive.

2.1.3.1 Laminated Object Manufacturing (LOM)

Laminated Object Manufacturing (LOM), which has been made and commercialzed by Helysis, is a RP strategy which produces three-dimensional models with foils of paper, plastic or composites. It could be seen as a hybrid between subtractive and included substance structures: the models are surely created with layers (like included substance structures), however every one layer is independently decreased by a laser (subtractive methodology) in the profile of the of the crosssection of the part [15].

The profiles are then trailed by an optics framework that is mounted to a X-Y stage. Unwanted material is trimmed into rectangles to encourage its later evacuation however remains in place during the build to act as supports. The sheets of papers are more far reaching than the part itself, so that when a cut is made its edges stay set up. In the wake of bringing down the part, the move of material could be progressed by slowing down abundance edges onto a second roller, hence the entire procedure might be rehashed. At the point when the part is made, it should be altered by the usage of epoxy sap spread or silicon fluid, to stay away from later contortion through water absorption.

The advantages of this system are (1) This technique uses the wide variety of modest materials, for example, paper, plastic or fiber-reinforced glass ceramics; (2) dimensions of the component, that may be look at significant contrasted with all the results of some other RP strategies;; (3) the rate which is 5-10 times greater than the other RP techniques.

The drawbacks is thecomplications experienced in uprooting the additional material. This leads to major problems ofdamages. An alternate imperative disadvantages is the necessity of theprecise environment loadedwith inactive gas extinguishersbecause of flame risks [16].

2.2 Application of RP method in biomedical engineering

In biomedical engineering, RP techniques are used for the fabrication of tissue engineering scaffold. Scaffold is a 3D matrix used as an implant on replacing the damaged tissue of the body. RP technologies are also applied in the medical/surgical domain for building models that provide visual and tactile information. In particular, RP models can be employed in the following applications [17].

- ***Operation planning*** **:** Using actual-size RP models of patients' pathological field, surgeons can more easily recognize the physical problems and achieve a better

approaching into the operations to be performed. RP objects can also assist surgeons in communicating with the proposed surgical procedures to patients.

- ***Surgery rehearsal*:** RP objects present exclusive opportunities for surgeons and surgical assistance to prepare for complex operations using the similar techniques and tools as in real surgery. These preparation can lead to changes in surgical procedures and considerably reduce risks.
- ***Prosthesis fabrication*:** RP objects can be used to fabricate objects which are then replicated using a biocompatible plastic material. Implants fabricated in this way are much more precise and economic than those formed with conventionally technique.

2.2.1 Use of RP technique in tissue engineering

Tissue engineering is a latest methodology which has the prospective to form tissues and organs de novo. It involves the features of in vitro seeding and attachment of human cells onto a scaffold. These cells then proliferate, migrate and differentiate into the particular tissue while secreting the extracellular matrix parts required to create the tissue. Present scaffolds, made by conventional scaffold fabrication techniques, are generally made from synthetic polymers. These cells do not necessarily identify such surfaces, and most significantly cells cannot migrate more than 600μm from the surface. The deficiency of the supply of oxygen and nutrient is the cause of this problem. Solid freeform fabrication (SFF) or Rapid prototyping techniques (RP) uses layer-by – layer fabrication methodology to build objects directly from computer-generated models. It can improve scaffold design by adjusting scaffold parameters such as pore size, porosity and pore distribution, as well as incorporating an artificial vascular system, thus increasing the mass transport of oxygen and nutrients into the periphery of the scaffold and sustaining cellular growth in that region [18].

2.3 Conspectus of the Fused Deposition Modeling (FDM) process

FDM technique was developed in the year 1989 and firstly commercialized in 1990 by Stratasys Inc. It is the second most extensively used rapid prototyping technology, after stereolithography. The method combines computer made it easier for pattern, chemical bonding of polymer, computer numerical mechanism, and also extrusion based systems to generate three dimensional (3D) solid objects straight from a model designed in the CAD software by using a layer by layer deposition of molten material having thermoplastics property to extruded through a minuscule nozzle. FDM process comprise of two portable heads (one for building the part and one for the backings) which store strings of liquid material onto a substrate. The material is warmed simply over its liquefying point so it solidifies promptly after expulsion and frosty welds to the past layers[19].

There are various important factors that affect the quality of part produced by FDM method of rapid prototyping but the most important are primarily the speed of deposition, layer thickness and resolution of the object fabricated. To examine the use of biodegradable polymer such as polymethylmethacrylate (PMMA) in fused deposition modelling (FDM) and to fabricate porous modified freeform structures for several applications including craniofacial reconstruction and orthopaedic spacers, an experiment was conducted by espalin et. al. It was found that a liquefier and covering temperature of 235 C and 55 C, respectively, as well as increasing the model feed rate by 60 percent, were necessary consistently extrude the PMMA filament. Structures with different porosities and fabrication conditions were produced, and their compressive mechanical properties were examined. Results showed that both the tip frequency and layer orientation used to fabricate the structures, as well as the porosity of the structure had an effect on the mechanical properties [20]. To improve the finish of the objects produced and to be able to use more variety of materials like ceramic materials, a lot of experiments has been done to improve the hardware

part of the process. To prototype a variety of ceramic components, a new process called FDC – Fused deposition of Ceramics was introduced by Allahverdi et al [21]. In this process objects were built by using polymer filaments loaded by ceramics.

A work was done by Anitha et. al. using Taguchi methods to study the most vital elements that effect the quality of structure fabricated from fused deposition modeling.The results showed that without pooling, only the layer thickness is effective to 49.4% at ninety five percent level of significance [22]. In an another experimental work done by L. M. Galantucci et. al. have determine the influence of FDM machining parameters on acrylonitrile butadiene styrene (ABS) prototype‟s fabricated objects. The objects fabricated after the modification of extrusion parameters has been measured and processed through designed experiments [23].

To apply the trial of new materials, new systems with different nozzles, like the multi nozzle system were brought in. A multi-nozzle is a bipolar deposition system having the capability of extruding living cells and bipolar solutions was developed by Khalil et al. [24], for the fabrication of a three dimensional freeform tissue scaffold. The final object built is also relatively dependent upon many essential factors, which includes the orientation of the deposition head. To build the object with good accuracy and finish, within the limits of built-up time and build cost, the ability to estimate the good quality object build and object orientation was quite important and was found by Xu et al [25].

CHAPTER 3 : MATERIALS & METHODS

3.1 Materials Name

- Polycaprolactone (PCL)- the rheological property was used for the mathematical and CFD analysis
- Brass- The rheological property of brass was used for the mathematical and CFD analysis
- Ansys – Fluent version 13.0 CFD software was used for analysis

3.2 Methods of modification in FDM technique

3.2.1 Physical Model :

The FDM device parameters that influence flow of metled material are the chamber temperature in which the scaffold is build, the volumetric rate flow of material in to the extrusion head and the temperature of the extrusion head. Uniformity and level of these parameters are essential in the fabrication of a proper scaffold [26].

The cylindrical tube section near the end of the extruder is known as the liquefier, which is joined with heating components that melt the polymer preceding extrusion (shown in figure 3.2) It ought to be cleared up that the liquefier is made of metal, and is covered in a layer of PTFE tape as an insulator to prevent thermal loss.

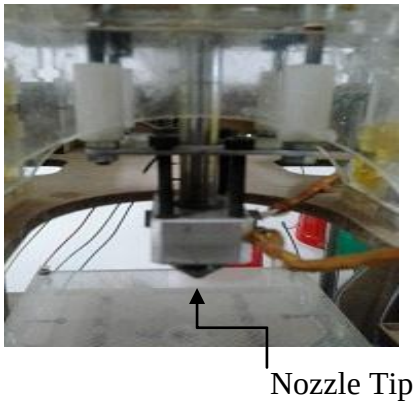

Figure 3.1: Extruder Part of FDM (Makerbot)

Figure 3.2 : Liquifier of the Nozzle.

The dynamic of the liquefier is also one of the most important component of the FDM device. In the liquefier the substantial system exhibits a complex behavior due to the unsteady flow of the viscous melting fluid. However, some more causes is responsible for this complex behavior that are as follows [2] :

- Fluid compressibility – The fluid used is non Newtonian i.e. shear stress is not directly proportional to the velocity gradient of fluid.
- Slip conditions between the walls of the liquifer and the flow of the melting material.
- The phase change of the material from solid to liquid is also an important factor.

Due to all these factor the fabricated scaffold is having some irregularities in their geometry and porosity. Thus, this research takes the fluid dynamics methodology to enhance the scaffold fabrication quality by the FDM process.This will be accomplished through examining the extruder subassembly. Polycaprolactone's melt flow behavior was analyzed using the Ansys 13.0 CFD software .

The building material taken for scaffold fabrication is Polycaprolactone (PCL), as it is presently preferred FDM thermopolymer. To clarify, the scaffold fabricated through the FDM process refers to the thickness and regularity of the PCL extrudate upon exit. These are the important parameters that constitutes the performance of the FDM process, and is directed by following three conditions [2],[27].

1. ***Melt flow temperature of PCL*** : It is essential not to extremely heated the PCL melt to an extremely high temperature which will results in increase of the fluidity, that will cause an extremely elongated length of the filament and unreliable diameter of the filament at the liquefier exit. This damages the surface completion of the fabricated scaffold.
2. ***Pressure Drop (ΔP)***: The pressure drop specifically influences the force needed to push the filament through. Adjusting the amount of force connected with the filament will

keep any development of material liquefy inside the liquefier which can result in an input impact, further increasing the pressure drop. Adjusting the force can retain the exit extruded melt as a steady stream with non-varying thicknesses. Any variations in layer thickness can contribute to overall imperfections in the design of the fabricated scaffold.

3. ***Existing diameter of the nozzle (d)*** : In order to keep a fine filament diameter, exiting diameter of the nozzle should be as lower as possible.

The melt flow temperature of PCL can be modified simply by modifying the boundary condition to improve the fabricated design of the scaffold. However, it is difficult for the nozzle existing diameter and for pressure drop. This is because the design of the scaffold fabricated finally , depends on both nozzle exiting diameter *(d)* and pressure drop *(ΔP)*.

On decreasing the value of nozzle existing diameter (*d)* excessively may compromise with the finally fabricated design of the scaffold instead of improving it. For example, if nozzle's existing diameter (*d*) is directly proportional to the fabrication process and inversely proportional to the pressure drop *(ΔP)*, an approach for optimizing the design of the scaffold fabrication is needed.

In this thesis the effect of varying nozzle diameter and nozzle angle on the pressure drop across the liquefier was sTudied both by mathematical modeling and by computational modelling (using Ansys – Fluent version 13.0 tool) and discuss the effect of pressure drop on the fabrication of scaffold.

- Original nozzle diameter ($d = 0.4\ mm$)
- Original nozzle angle ($\alpha = 120°$)

3.2.2 Mathematical Model

A numerical model was developed for evaluating the pressure drop at the exiting nozzle tip of the liquefier. The compressive force applied on the filament of the PCL has to overcome the

pressure drop in the liquefier. The compressive force applied on the filament of the PCL is through a nail driven by a motor, when torque is developed on the rotation of the motor.

The numerical relation between the compressive force, F and the torque, T_d developed in the motor is [28] :

$$T_d = \frac{F}{2} \times R_s$$

With relation of the torque, T_d and power, P is [29] :

$$P = T_d \times \omega$$

Where R_s is the radius of the shaft of the motor and ω be the angular velocity of the motor (i.e. RPM of the motor). This numerical model defines the relationship between the pressure drop (ΔP) across the liquefier.

For deriving the mathematical concept, geometry of the liquifier must be divided into three section having height H_1, H_2 and H_3 respectively (see Figure 3.1). Every section has a unique equation for evaluating pressure drop for its specific geometry. The summation of all the three pressure drop is the overall pressure drop at the exiting nozzle diameter of the liquefier.

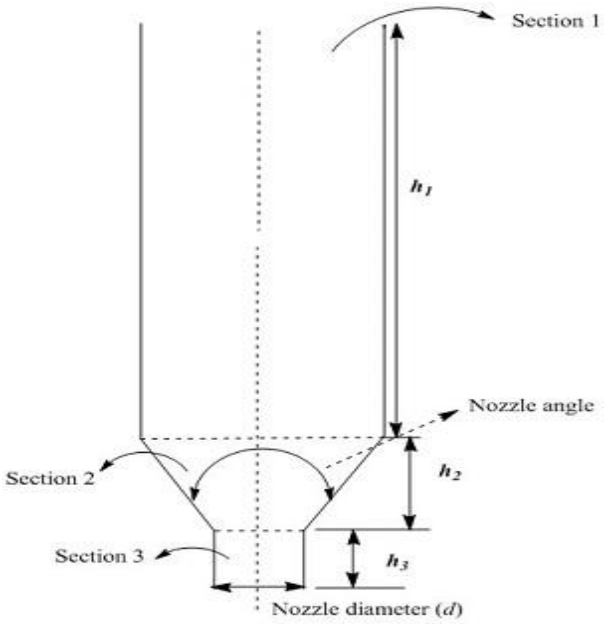

Figure 3.3: Section wise representation of the geometry of the nozzle for mathematical modeling

Assumption required to derive the mathematical equation [30], [31] :

- ***Steady state fluid flow*** : Steady-state flow defines the condition where the fluid properties at a point in the control volume does not change with time.
- ***Isothermal fluid flow*** : all the molecules of the fluid are at same temperature throughout the flow.
- The fluid should not be compressible i.e. incompressible fluid (density remains constant)
- The velocity of flow of the fluid does not change in the direction of flow (i.e. hydrodynamically fully developed flow).

  Thus, velocity of fluid flow in the x-drection is shown below :

$$\frac{du}{dx} = 0$$

- Gravity effect should be neglected.
- Velocity of the fluid at the wall of the liquefier is equal to zero (i.e. no slip condition of fluid mechanics).

- No need of external force required because the motor provides the sufficient force to push the filament in the liquefier.

Derivation for evaluating the pressure drop across section 1 :

The derivation begins by using the Navier's – stoke equation (momentum flux equation) for a differential cylindrical control volume with thickness dr and axial length of dh (see Figure 3.2). Since the fluid flow with constant velocity, that does not affected by the direction of flow.Also, the fluid is assumed to be incompressible, the Navier's stoke equation has only the force balance part.

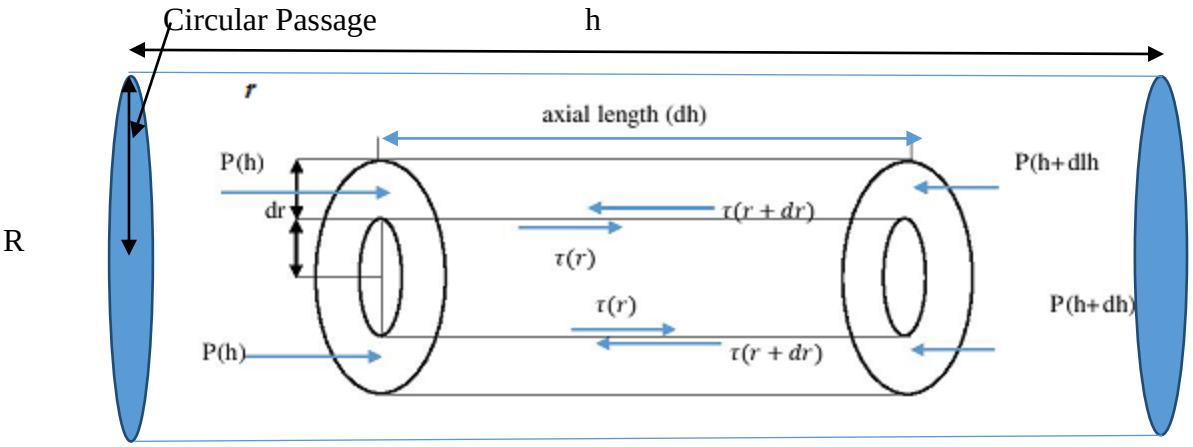

Figure 3.4 : Schematic representation of the force balance phenomenon in a cylindrical control volume (Source : [30]).

$2\pi r dr\,[p(h) - p(h+dh)] + \tau(r)2\pi r dh - \tau(r+dr)\,.2\pi\,(r+dr)dh = 0$.....(1)

By using the Taylor's series phenomenon, we get :

$$p(h+dh) = p(h) + \frac{\partial p}{\partial h}dh \text{.....(a)}$$

$$\tau(r+dr) = \tau(r) + \frac{\partial \tau}{\partial r}dr \text{.....(b)}$$

On substituting eq. (a) and (b) in eq. (1), the modified eq. is

$$2\pi r dr\ \left[p(h) - p(h) - \frac{\partial p}{\partial h} dh\right] + \ \tau(r) 2\pi r dh - \tau(r) - \ \frac{\partial \tau}{\partial r} dr\ .2\pi\ \ (r + dr) dh = 0$$

On simplifying the above equation, the resulting expression is as:

$$-r\ \frac{\partial p}{\partial h} - \left(\tau + \frac{\partial \tau}{\partial r} r + \frac{\partial \tau}{\partial r} dr\right) = 0 \text{……..(2)}$$

Since the flow of the fluid is the hydrodynamically developed, so,the rate at which pressure changes for a particular location (i.e. pressure gradient) remains constant with respect to the pressure drop across the cylinder and total length of the circular cross-section of the cylinder *h*. Thus, it signifies that rate of change in pressure drop with length of the circular cross-section of cylinder h :

$$\frac{\partial p}{\partial h} = \frac{\Delta p}{h}$$

On substituting the above relation in eq. (2), the resulting expression is as :

$$-r \frac{\Delta p}{h} - \left(\tau + \frac{\partial \tau}{\partial r} r + \frac{\partial \tau}{\partial r} dr\right) = 0$$

$$-r \frac{\Delta p}{h} = \ \tau + \frac{\partial \tau}{\partial r} r + \frac{\partial \tau}{\partial r} dr$$

$$\frac{\Delta p}{h} = -\frac{\tau}{r} - \frac{\partial \tau}{\partial r} - \frac{\partial \tau}{\partial r} dr . \frac{1}{r}$$

$$\frac{\Delta p}{h} = -\frac{\tau}{r} - \frac{\partial \tau}{\partial r}\left(\frac{r + dr}{r}\right) = -\frac{\tau}{r} + \frac{\partial \tau}{\partial r} + 2\frac{\partial \tau}{\partial r}$$

$$\frac{\Delta p}{h} = \frac{\partial \tau}{\partial r} + \frac{\tau}{r}$$

Firslty, finding the integrating factor for above equation, it is :

$$I.F. = e^{\int \frac{1}{r} dr} = e^{ln\ r} = \frac{1}{r}$$

Now, on solving the above equation using the first order differential equation method, the results shows the shear stress across section 1 :

$$\tau \times I.F = \int \frac{\Delta p}{h} \times I.F\ dr + C$$

Thus,

$$\frac{\tau}{r} = \frac{\Delta p}{h} \times \frac{r^2}{2} + C$$

$$\tau = \frac{\Delta p}{2h} \times r + \frac{C}{r}$$

On appliying the boundary condition that if r tends to zero , then there will be no shear force hence *C* becomes zero gives the relation :

$$\tau = \frac{\Delta p}{2h} \times r \ldots\ldots (3)$$

The material flow behavior is an important factor for shear stress, but the above equation does not consider it since the fluid (PCl) used here is non-newtonian in nature. To optimize the material flow behavior, power law equation can be used that defines the deviance of the PCl fluid from the Newtonian fluid[26].

The power law equation also known as Ostwald – de –waele relationship [32], [33] can be expressed as :

$$\tau = k\left(-\frac{\partial v}{\partial r}\right)^n \ldots\ldots\ldots\ldots (c)$$

Where,

- *K* is the *flow consistency index* (SI units Pa•s^n),
- *∂v*/*∂r* is the shear rate or the velocity gradient perpendicular to the plane of shear (SI unit s^{-1}), and
- *n* is the *flow behavior index* (dimensionless).

The term;

$$\mu = k\left(-\frac{\partial v}{\partial r}\right)^{n-1} \ldots\ldots\ldots\ldots (d)$$

refers the effective viscosity as a function of the shear stress.

If the following substitution have done :

$$n = \frac{1}{m}$$

$$k = \emptyset^{-1/m}$$

The modified expression for the eq.(c) and eq. *(d*), is as:

$$\tau = k \times \left(-\frac{\partial v}{\partial r}\right) \ldots\ldots\ldots\ldots\ldots (e)$$

$$\mu = \emptyset^{-1/m} \left(-\frac{\partial v}{\partial r}\right)^{\frac{1-m}{m}} \ldots\ldots\ldots (f)$$

On comparing eq.*(e)* and eq.*(f)* in above eq. the expression is :

$$\tau = \emptyset^{-1/m} \left(\frac{\partial v}{\partial r}\right)^{\frac{1-m}{m}} \times \left(\frac{\partial v}{\partial r}\right) = \left(\frac{1}{\emptyset}\right)^{1/m} \times \left(-\frac{\partial v}{\partial r}\right)^{1/m} \ldots\ldots\ldots (g)$$

On substituting this modified form of power law equation in eq.*(3)*, the modified eq. is as :

$$\frac{\Delta p}{2h} \times r = \left(\frac{1}{\emptyset}\right)^{1/m} \times \left(-\frac{\partial v}{\partial r}\right)^{1/m}$$

$$\frac{\partial v}{\partial r} = -\emptyset \left(\frac{\Delta p}{2h} r\right)^{m}$$

The integrating of the above equation, gives the result that represent velocity of the fluid at radius ‘r’ of any control volume of the cylinder.

$$v = -\emptyset \left(\frac{\Delta p}{2h}\right) \int r^m \, dr == -\emptyset \left(\frac{\Delta p}{2h}\right) \times \frac{r^{m+1}}{m+1} + C \ldots\ldots (4)$$

Since,we have taken the assumption of no-slip condition, the velocity at the wall of the cylindrical wall is zero , and if we take another boundary condition [i.e.internal radius of the nozzle (*r)* is equal to the radius of circular cross –section (R) :

$$r = R$$

Then, constant '*C*'

$$C = \emptyset\left(\frac{\Delta p}{2h}\right) \times \frac{R^{m+1}}{m+1}$$

On substituting the value of constant *'C'*in eq. (4) we get

$$v = \emptyset\left(\frac{\Delta p}{2h}\right)\frac{R^{m+1} - r^{m+1}}{m+1}$$

The average velocity of the fluid in all the three section of the nozzle is calculated as :

$$\dot{v} = \emptyset\left(\frac{\Delta p}{2h}\right) \times \frac{{r_i}^{m+1}}{m+3}$$

After simplifying the above equation, the resulting expression for the pressure drop is :

$$\Delta p = 2h\left(\frac{\dot{v}}{\emptyset}\right)^{1/m} \times \frac{m+3}{{r_i}^{m+1}}$$

Also,

$$\eta = \mathrm{H(T)} \cdot \eta_0(\gamma)$$

From Arrhenius equation , viscosity is related to the temperature as ,at no shear stress, we considered the properties of PCL as a Newtonian fluid [34], [35]:

$$\mathrm{H}(T) = exp\left[E_a\left(\frac{1}{T - T_a} + \frac{1}{T_0 - T_a}\right)\right]$$

T_a = 0 for absolute temperature

T_0 is the temperature at which $\emptyset$ and m are calculated for which H *(T)* = 1

By using the Arrhenius equation; the pressure drop across section 1 is as :

$$\Delta p_1 = 2h_1\left(\frac{\dot{v}}{\emptyset}\right)^{1/m} \times \frac{m+3}{{r_i}^{m+1}} \times exp\left[E_a\left(\frac{1}{T - T_a} + \frac{1}{T_0 - T_a}\right)\right]$$

Similarly the expression of the derivation for section 2 and section 3 by using the assumption of slightly low Reynold's number (since the flow is laminar) [1]

$$\Delta p_2 = \frac{2m}{3tan\frac{\alpha}{2}}\left(\frac{1}{r_e^{\frac{3}{m}}} - \frac{1}{r_i^{\frac{3}{m}}}\right) \times \left(\frac{\dot{v}}{\emptyset}\right)^{\frac{1}{m}} \times [r_i{}^2.2^{m+3}.(m+3)]^{1/m} \times exp\left[E_a\left(\frac{1}{T-T_a} + \frac{1}{T_0-T_a}\right)\right]$$

$$\Delta p_3 = 2h_3 \times \left(\frac{\dot{v}}{\emptyset}\right)^{\frac{1}{m}} \times \left(\frac{r_i{}^2.(m+3)}{r_e{}^{m+3}}\right) exp\left[E_a\left(\frac{1}{T-T_a} + \frac{1}{T_0-T_a}\right)\right]$$

The pressure drop at the tip of the nozzle should be calculated by the summation of all the pressure drop of the respective section.

$$\Delta p = \Delta p_1 + \Delta p_2 + \Delta p_3$$

Table no.1: PCL rheological properties taken for the mathematical simulation [36] :

S.no.	***Property***	***Symbol***	***Values***	***Unit***
1.	Viscosity	η	0.283	mPa-s
2.	Temperature	T_0	403.15	Kelvin (K)
3.	Temperature	T	339	Kelvin (K)
4.	Inlet velocity of the PCL filament	V	0.002	m/s

Table no. 2 : Specification of the Nozzle for mathematical simulation :

S.no.	***Nozzle inlet diameter (D)mm***	***Nozzle extruded diameter (d)mm***	***Nozzle Angle (α)***	***Nozzle Length (h) mm***
1.	3	0.5	120^o	71.221709
2.	3	0.4	120^0	71.251
3.	3	0.3	120^0	71.27944
4.	3	0.2	120^0	71.308314

5.	3	0.5	90^0	71.75
6.	3	0.4	90^0	71.8
7.	3	0.3	90^0	71.85
8.	3	0.2	90^0	71.75
9.	3	0.5	60^0	72.665
10.	3	0.4	60^0	72.7516
11.	3	0.3	60^0	72.8382
12.	3	0.2	60^0	72.9248

With the above specification, value of pressure drop at the tip of the nozzle on various nozzle angle and nozzle diameter can be calculated and described in chapter no. 4.

3.2.3 CFD Model

Polycaprolactone (PCL) is a thermoplastic fluid, having the properties that viscosity decreases with the increase in shear rate, which reduces the Reynold's number less than 1. Thus, viscous forces influence the inertial forces at this small range, and was predictable that there would be a variation in pressure drop by varying nozzle parameters such as nozzle angle and nozzle diameter. A total of twelve cases were examined using Ansys – fluent 13.0 version software and graphs were plotted between nozzle angle vs. pressure and nozzle diameter vs. pressure drop. Same table no. 2 specification is used for the purpose of drawing the geometry of the liquifier and the required boundary condition and the rheologcal properties required for the CFD analysis is shown in Table 3, 4, 5 respectively :

Table no. 3 : Boundary conditions required for the CFD analysis :

S.no.	***Name of the boundary condition***	***Values***	***Units***
1.	Inlet velocity of the PCl filament	0.002	m/s
2.	Temperature at inlet	298	Kelvin (K)
3.	Left wall temperature	339	Kelvin (K)
4.	Right wall temperature	339	Kelvin (K)
5.	Left tapered wall temperature	339	Kelvin (K)
6.	Right tapered wall temperature	339	Kelvin (K)
7.	Left small wall temperature	339	Kelvin (K)
8.	Right small wall temperature	339	Kelvin (K)
9.	Back flow temperature at outlet	298	Kelvin (K)

Table no. 4 : Rheological properties of PCL required for CFD simulation

S.no.	***Property***	***Values***	***Units***
1.	Viscosity	0.283-0.595	mPa-s
2.	Density	1.145	g/cm^3
3.	Thermal conductivity	0.14	w/m-k
4.	Specific heat	1.34	KJ/Kg at 25^oC

Table no. 5 : Rheological properties of Brass required for CFD simulation

S.no.	***Property***	***Values***	***Units***
1.	Density	8525	Kg/cm^3
2.	Thermal conductivity	380	w/m-k
3.	Specific heat	110.784	J/Kg

Chapter 4 : Results & Discussion

4.1 Results and Discussion

4.1.1 Pressure Drop calculation at different nozzle parameters – based on mathematical analysis

The pressure drop equation were solved for the original nozzle specifications (0.4 mm nozzle diameter and 120 degree nozzle angle) also for three other nozzle diameter with varying nozzle angle. The results in figure 4.1 shows that pressure drop increasing by reducing the nozzle angle and nozzle diameter. Later, the result was compared with the CFD model in section 4.2.

Table no. 6 : Pressure Drop (kPa) calculation on various parameters a) Nozzle Diameter, b) Nozzle Angle

S.no.	***Nozzle Angle (Degree)***	***Nozzle Diameter (mm)***	***Pressure Drop (kPa)***
1.	60	0.5	114.2385
2.	60	0.4	174.6854
3.	60	0.3	283.6815
4.	60	0.2	592.5693
5.	90	0.5	112.3592
6.	90	0.4	164.7983
7.	90	0.3	278.4313
8.	90	0.2	574.7931

9.	120	0.5	109.83567
10.	120	0.4	161.6271
11.	120	0.3	266.8143
12.	120	0.2	568.8125

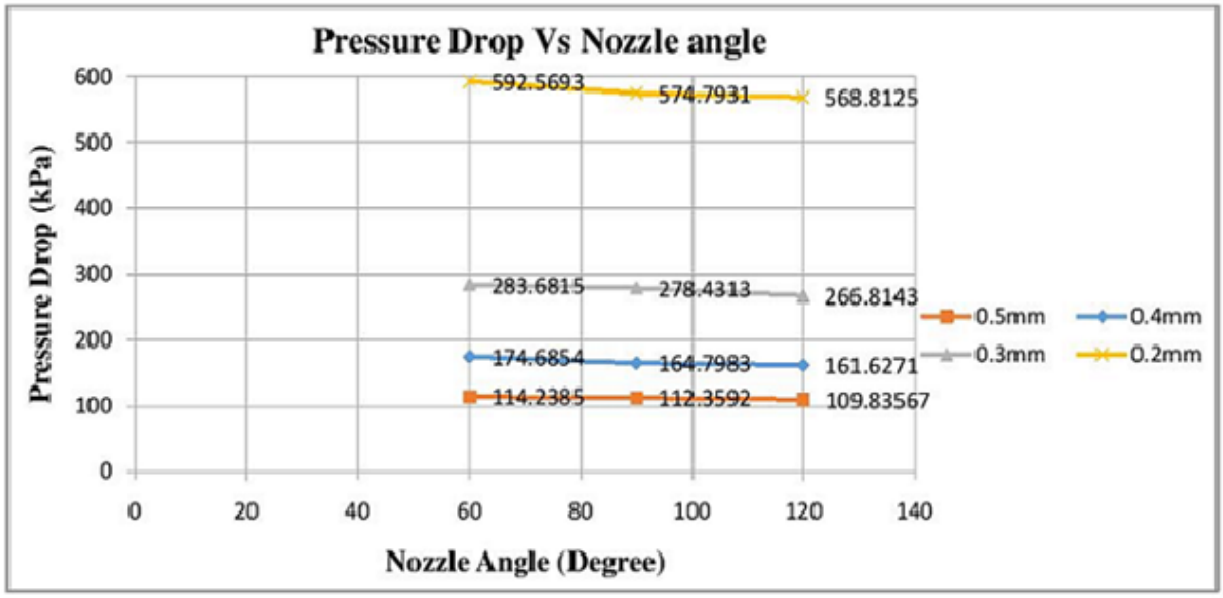

Figure 4.1 : Mathematical analysis : Pressure Drop vs Nozzle Angle (at different nozzle diameter).

The above figure shows the pressure drop calculation at varying nozzle angle for a particular nozzle diameter by using the mathematical analysis. It can be studied that the pressure drop was lowest for nozzle angle of 120 degree for all the varying nozzle diameter. Hence, it is clear that on raising the nozzle angle the pressure drop goes on decreasing. The higher pressure is the important parameter for the resolution of the geometry of the fabricated scaffold.

4.2 Pressure Drop calculation at different nozzle parameters – based on CFD analysis

The CFD model was simulated using Ansys-Fluent 13.0 version software for varying nozzle angle and nozzle diameter and the respective pressure drop was estimated.The resulting pressure drop calculated here is shown in Table no. 7. Later it studied and comapare with the original dimension of the FDM machine (0.4 mm nozzle diameter and 120 degree nozzle angle) in the chapter 4.3.

Table no. 7 : Pressure Drop (kPa) calculation on various parameters a) Nozzle Diameter, b) Nozzle Angle

S.no.	***Nozzle Angle (Degree)***	***Nozzle Diameter (mm)***	***Pressure Drop (kPa)***
1.	60	0.5	102.39843
2.	60	0.4	149.2055
3.	60	0.3	255.99837
4.	60	0.2	557.28332
5.	90	0.5	97.285487
6.	90	0.4	147.90799
7.	90	0.3	251.36971
8.	90	0.2	553.15387
9.	120	0.5	94.092265
10.	120	0.4	140.83076
11.	120	0.3	245.136742
12.	120	0.2	547.69009

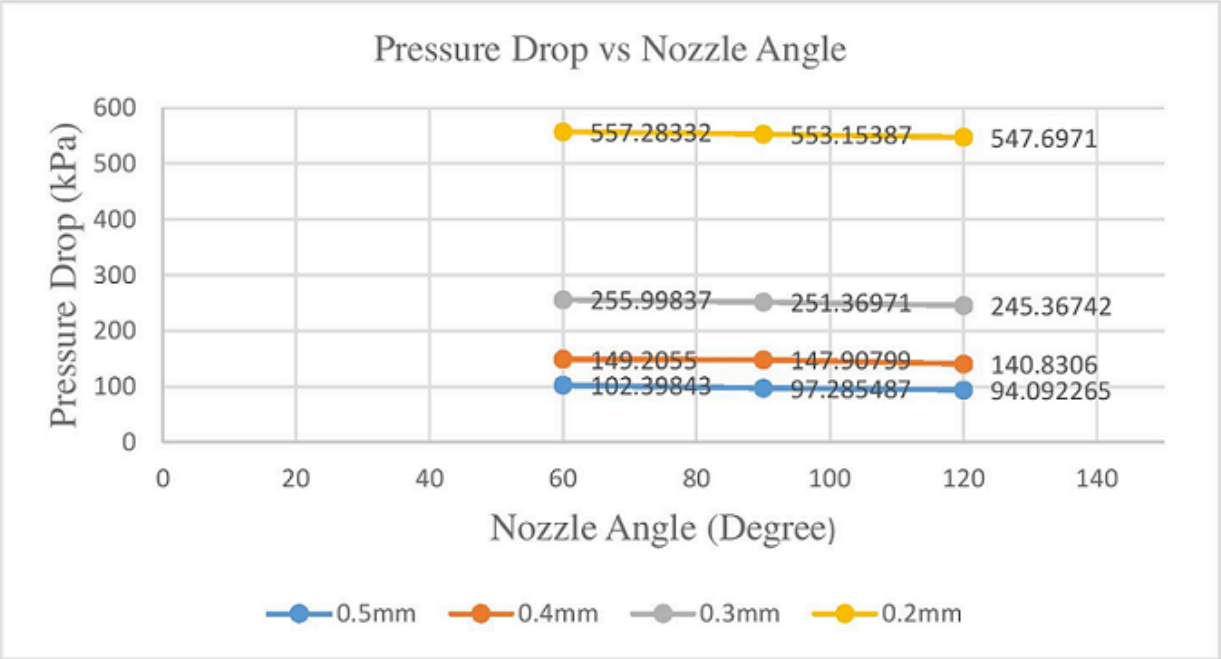

Figure 4.2 : CFD analysis : Pressure Drop vs Nozzle Angle (at different nozzle diameter).

Figure 4.2 shows above give the same result as examined using mathematical analysis of the calculation of pressure drop at varying nozzle angle for a particular nozzle diameter using the CFD analysis . It results showed that the pressure drop was lowest for nozzle angle of 120 degree for all the varying nozzle diameter.

Moreover, it can be seen that for in figure 4.1 and 4.2 (at a different nozzle diameter), the slope of these lines (or the rate of change) of ΔP increases with increasing d in all cases. But also estimated that at lower nozzle diameters, on taking the nozzle angle from 60^0 to 120^0 resulted in slightly small changes in pressure drop than those of higher nozzle diameters. Therefore, at lower nozzle diameters, modifying the nozzle angle will not so much effect on the pressure drop across the liquefier.

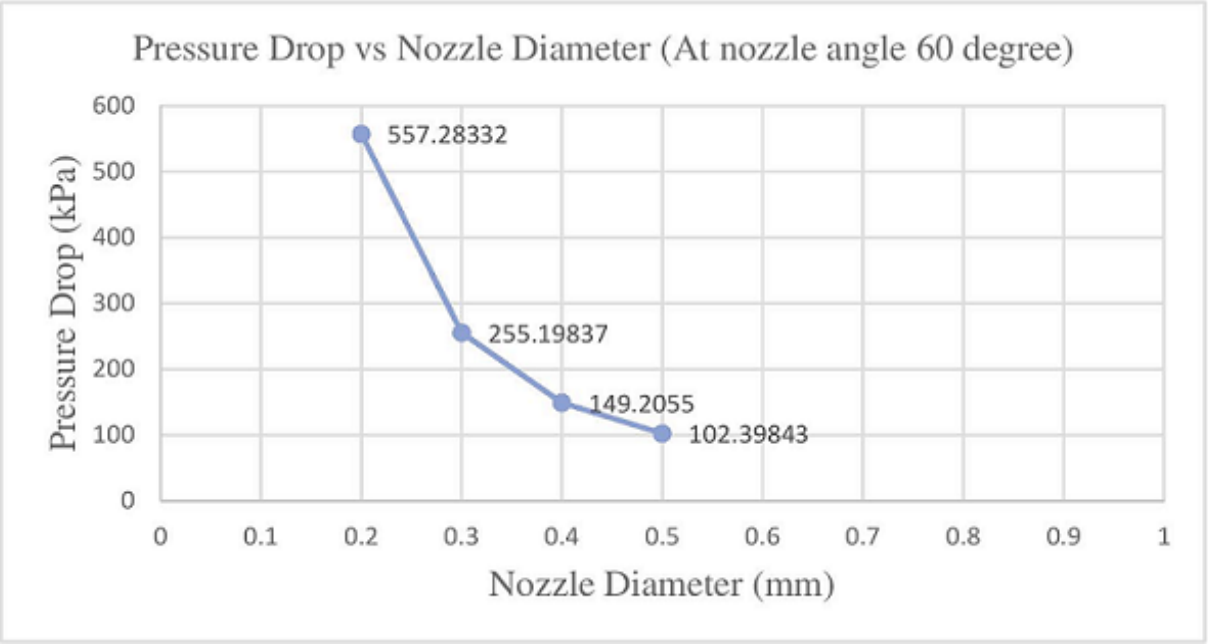

Figure 4.3 : CFD analysis : Pressure Drop vs Nozzle Diameter (at nozzle angle 60 degree)

The above figure shows the decrease in pressure drop with increase in nozzle diameter at nozzle anglof 60 degree.

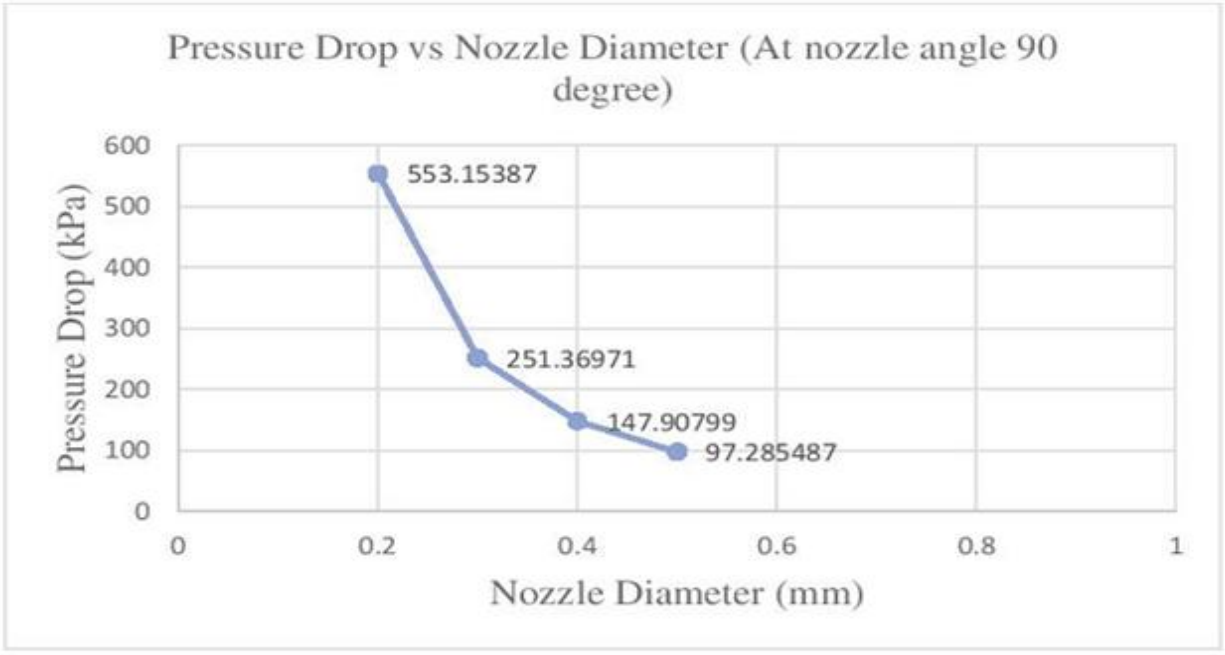

Figure 4.4 : CFD analysis : Pressure Drop vs Nozzle Diameter (at nozzle angle 90 degree).

The above figure shows the decrease in pressure drop with increase in nozzle diameter at nozzle at nozzle angle 90 degree.

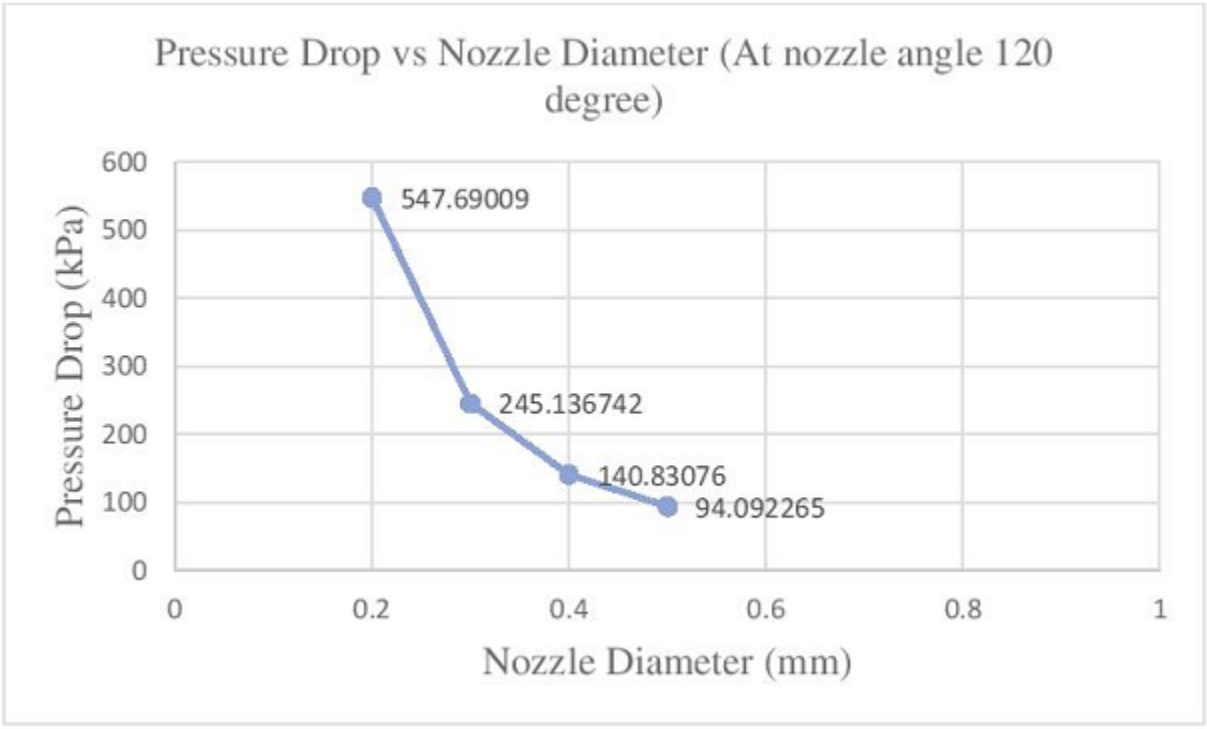

Figure 4.5 : CFD analysis : Pressure Drop vs Nozzle Diameter (at nozzle angle 120 degree).

It can also be seen in figure 4.3 , figure 4.4 and figure 4.5 that from nozzle diameter 0.5 mm to 0.3 mm there was a change of 152.79994, 154.084223, 151.044477 (kPa) in the pressure drop respectively at different nozzle angle, but from nozzle diameter 0.3mm to 0.2 mm there was a more abrupt changes of 302.08495, 301.78416, 302.553348 (kPa) in the pressure drop almost double that changes from nozzle diameter 0.5 mm to 0.3 mm.So, it can be studied that setting nozzle diameter = 0.3 mm provides a overall greater resolution in the fabrication rather than nozzle diameter of 0.2 mm at such a high pressure drop. Such high of the pressure needed high torque to be produced by the motor. That also raises the cost of the machine.

4.3. Comparison of the Mathematical analysis with the CFD analysis

The analysis of the mathematical model was compared with the CFD model for further use this analysis experimentally.

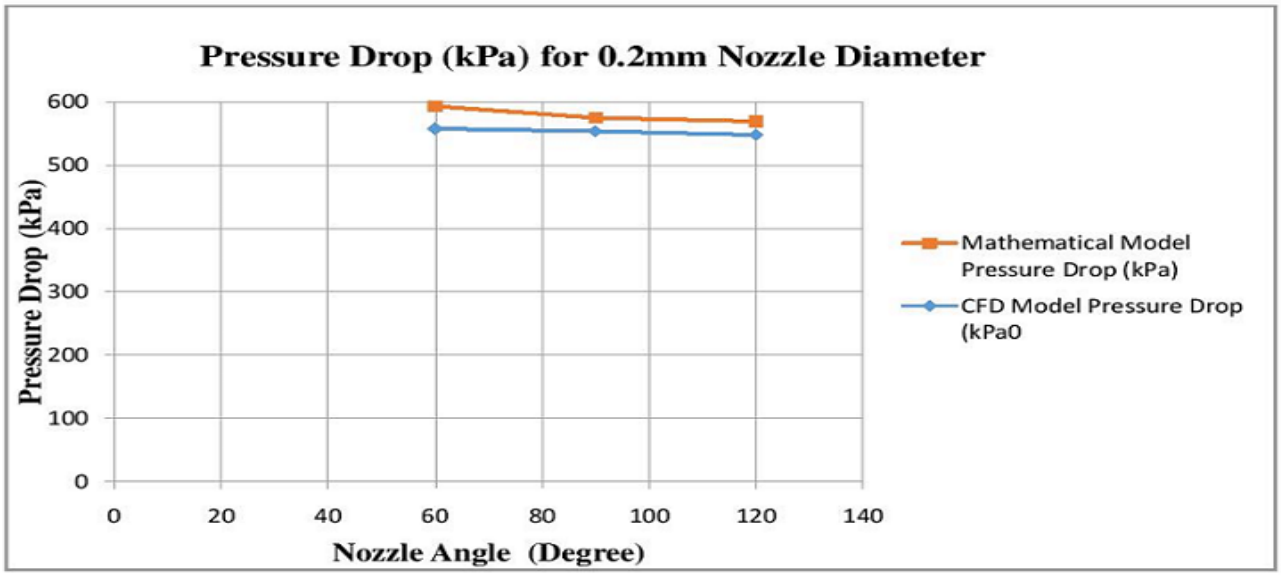

Figure 4.6 : Comparison of the pressure drop estimated in Mathematical analysis and CFD analysis at 0.2 mm nozzle diameter.

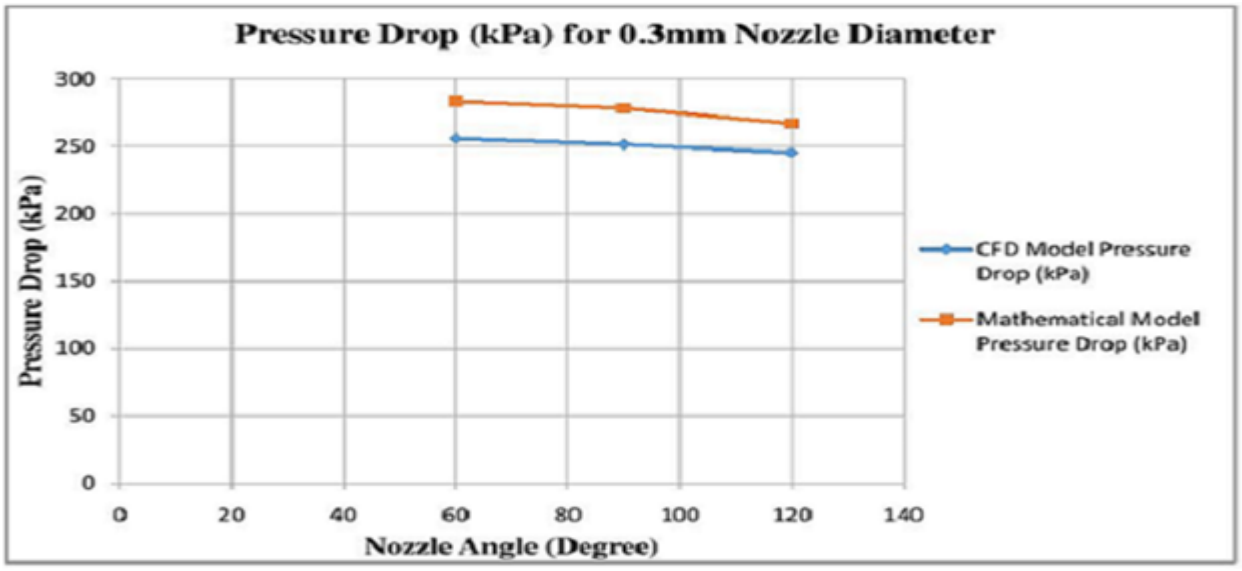

Figure 4.7 : Comparison of the pressure drop estimated in Mathematical analysis and CFD analysis at 0.3 mm nozzle diameter.

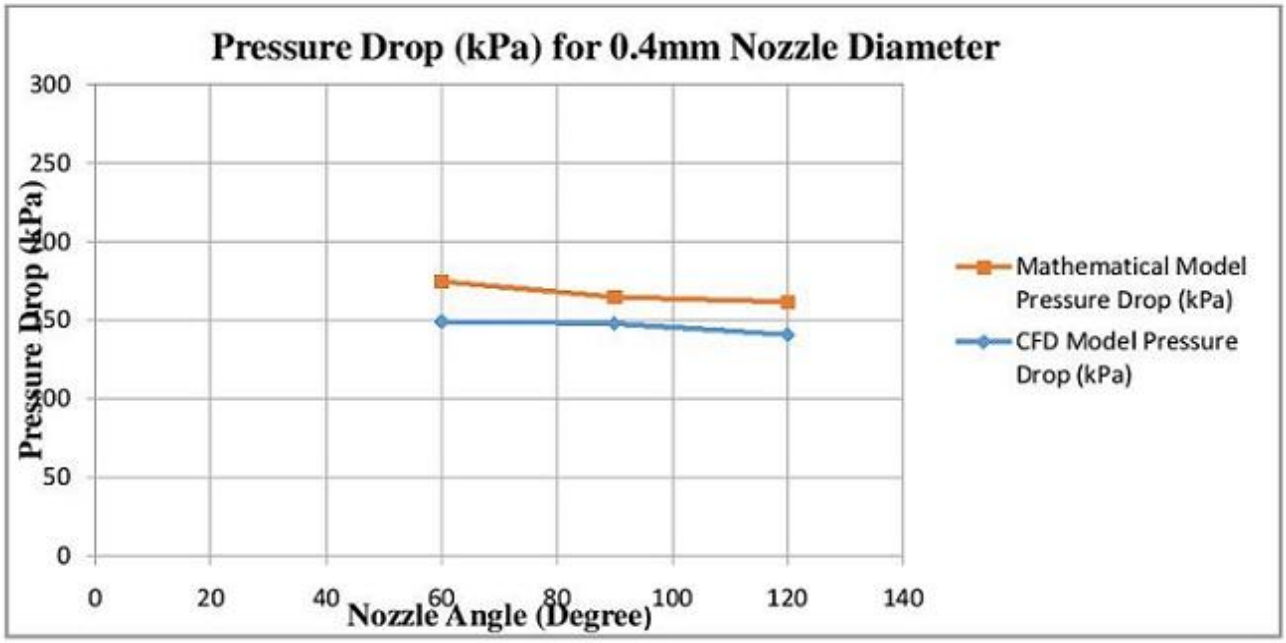

Figure 4.8 : Comparison of the pressure drop estimated in Mathematical analysis and CFD analysis at 0.4 mm nozzle diameter.

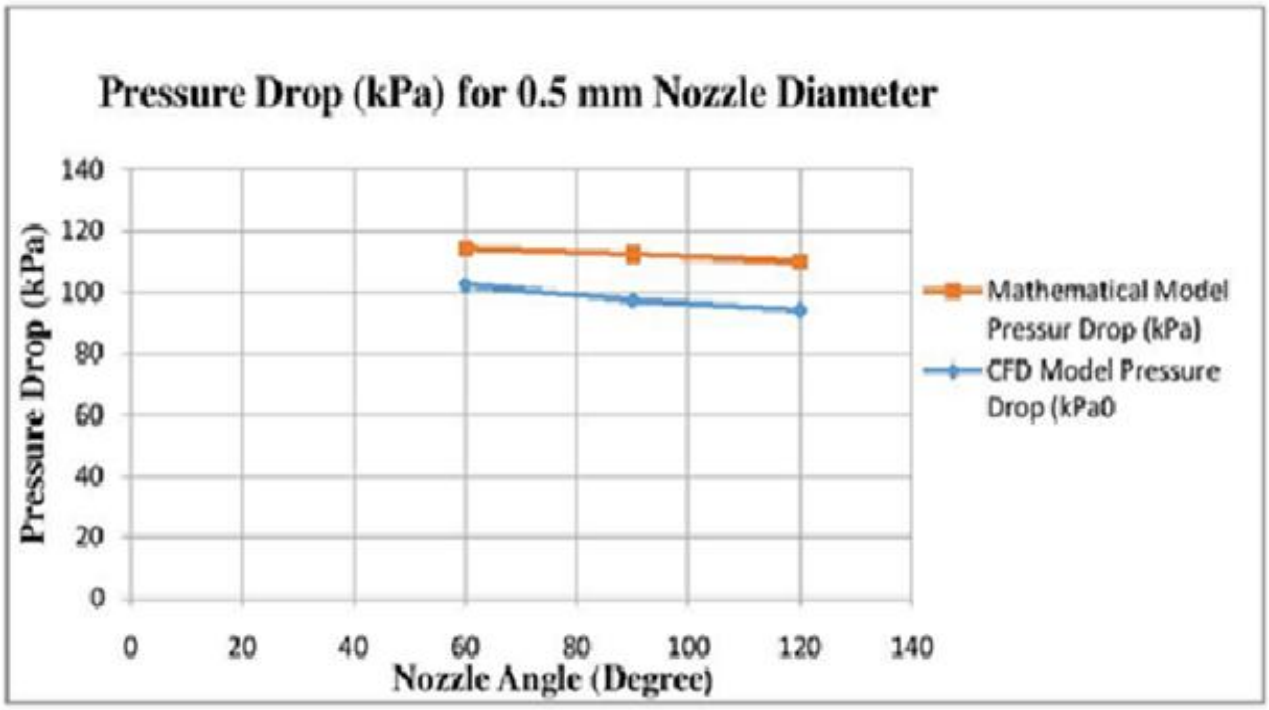

Figure 4.9 : Comparison of the pressure drop estimated in Mathematical analysis and CFD analysis at 0.5 mm nozzle diameter.

Under the work done by the Bellini the variation between the mathematical and CFD analysis was comparatively high [2].The above four figures (4.6-4.9) shows the slightly minute (aprrox.

6-10%) variations in the these two analysis. It is due to the fact, that the mathematical results were defined by deriving the three mathematical equation of the pressure drop.These equations are based on the parameters that associated with the geometry of the liquefier, rheological properties of the Polycaprolactone, and on the temperature.

Moreover, the significant limitation to using the mathematical model was that it inaccurately assumes isothermal conditions throughout the total length of the liquefier while the CFD model did not since the temperature at the time of entering the PCl filament in the liquefier did not instantly change to the inner wall temperature of 339K.

CHAPTER 5 : CONCLUSION

In conclusion, the flow behaviour of melted PCL in the liquifier of the FDM has been examined by studying the pressure drops at various nozzle diameter and nozzle angle. Two methods were used to study the melt flow behaviour. First, by mathematical modelling and second with CFD model using Ansys-Fluent version 13.0 software. Also, the affect of pressure drop on the fabrication of scaffold was studied. The pressure drops at three sections were obtained for four different nozzle diameters, 0.2, 0.3, 0.4 mm and 0.5mm by varying the nozzle angles from 60,90 and 120 degree. The mathematical and CFD analysis results showed that the nozzle diameter and nozzle angle variation effect directly on the pressure drop.

From the results obtained, the design of the Makerbot extruder can accommodate a decrease in the nozzle diameter with utilizing the same material (PCL) without any adverse effects. The proposed redesign suggests the nozzle diameter should be decreased to 0.3 mm,since higher pressure drop at small nozzle diameter leads to continuous flow of the material from the extruder. This helps in the fabrication of scaffold with fine geometry and proper orientation. A study on 0.2 mm diameter concealed that the pressure drop was too high for a reasonable cost of the motor to be able to produce the necessary force requisite to push the filament through the liquefier.

FUTURE PROSPECTS

Future Prospects

This study was a simplified case where the fluid flow is steady and continuous which would be suitable, if the device created one long continuous material road layer during the experiment. But, in actual practice, the flow is non-continuous and unsteady because there are breaks between each layer and material road .Moreover, development of a material road built on top of previous layers will subsequently cause a change in the actual road's dimensions. A novel method was developed that explores these non-simplified cases for further study.

The analysis done in this study focused mainly on CFD model. On comparing of CFD model with mathematical model, the result shown that mathematical model has adverse effects related to scaffold fabrication process. Therefore, there was more assurance in using the CFD model to optimize liquefier parameters. Further research is yet to be done to continue with CFD method unless a more stable and conservative mathematical model can be developed to better illustrate the problem. Further experimental study is required to examined the exit melt flow utilizing a 0.3mm nozzle diameter as a suggested improvement from CFD analysis.

REFERENCES

[1] S. Yang, *et al.*, "The design of scaffolds for use in tissue engineering. Part II. Rapid prototyping techniques," *Tissue Engineering*, vol. 8, pp. 1-11, 2002.

[2] A. Bellini, *et al.*, "Liquefier dynamics in fused deposition," *Journal of Manufacturing Science and Engineering*, vol. 126, pp. 237-246, 2004.

[3] V. A. Raghu, "An investigation into curved layer deposition for Fused Deposition Modelling," AUT University, 2010.

[4] P. F. Jacobs, *Stereolithography and other RP&M technologies: from rapid prototyping to rapid tooling*: Society of Manufacturing Engineers, 1995.

[5] K.-W. Lee, *et al.*, "Poly (propylene fumarate) bone tissue engineering scaffold fabrication using stereolithography: effects of resin formulations and laser parameters," *Biomacromolecules*, vol. 8, pp. 1077-1084, 2007.

[6] D. Pham and R. Gault, "A comparison of rapid prototyping technologies," *International Journal of Machine Tools and Manufacture*, vol. 38, pp. 1257-1287, 1998.

[7] C. K. Chua, *et al.*, *Rapid prototyping: principles and applications*: World Scientific, 2010.

[8] R. Noorani, *Rapid prototyping: principles and applications*: John Wiley & Sons Incorporated, 2006.

[9] F. Wiria, *et al.*, "Poly-< i> ε</i>-caprolactone/hydroxyapatite for tissue engineering scaffold fabrication via selective laser sintering," *Acta Biomaterialia*, vol. 3, pp. 1-12, 2007.

[10] K. Dalgarno and T. Stewart, "Manufacture of production injection mould tooling incorporating conformal cooling channels via indirect selective laser sintering," *Proceedings of the Institution of Mechanical Engineers, Part B: Journal of Engineering Manufacture*, vol. 215, pp. 1323-1332, 2001.

[11] http://www.egr.uri.edu/ime/RMC/lens.html.

[12] T. Hanemann, *et al.*, "Rapid prototyping and rapid tooling techniques for the manufacturing of silicon, polymer, metal and ceramic microdevices," in *MEMS/NEMS*, ed: Springer, 2006, pp. 801-869.

[13] J. Zhao, *et al.*, "Research on laser engineered net shaping of thick-wall nickel-based alloy parts," *Rapid Prototyping Journal*, vol. 15, pp. 24-28, 2009.

[14] D. Dimitrov, *et al.*, "Advances in three dimensional printing-state of the art and future perspectives," *Journal for New Generation Sciences*, vol. 4, pp. p. 21-49, 2006.

[15] B. Mueller and D. Kochan, "Laminated object manufacturing for rapid tooling and patternmaking in foundry industry," *Computers in Industry,* vol. 39, pp. 47-53, 1999.

[16] M. Feygin and S. S. Pak, "Laminated object manufacturing apparatus and method," ed: Google Patents, 1999.

[17] L. Hieu, *et al.*, "Medical rapid prototyping applications and methods," *Assembly Automation,* vol. 25, pp. 284-292, 2005.

[18] E. Sachlos and J. Czernuszka, "Making tissue engineering scaffolds work. Review: the application of solid freeform fabrication technology to the production of tissue engineering scaffolds," *Eur Cell Mater,* vol. 5, pp. 39-40, 2003.

[19] P. Pandey, *et al.*, "Real time adaptive slicing for fused deposition modelling," *International Journal of Machine Tools and Manufacture,* vol. 43, pp. 61-71, 2003.

[20] D. Espalin, *et al.*, "Fused deposition modeling of patient-specific polymethylmethacrylate implants," *Rapid Prototyping Journal,* vol. 16, pp. 164-173, 2010.

[21] M. Allahverdi, *et al.*, "Processing of advanced electroceramic components by fused deposition technique," *Journal of the European Ceramic Society,* vol. 21, pp. 1485-1490, 2001.

[22] R. Anitha, *et al.*, "Critical parameters influencing the quality of prototypes in fused deposition modelling," *Journal of Materials Processing Technology,* vol. 118, pp. 385-388, 2001.

[23] L. Galantucci, *et al.*, "Experimental study aiming to enhance the surface finish of fused deposition modeled parts," *CIRP Annals-Manufacturing Technology,* vol. 58, pp. 189-192, 2009.

[24] S. Khalil, *et al.*, "Multi-nozzle deposition for construction of 3D biopolymer tissue scaffolds," *Rapid Prototyping Journal,* vol. 11, pp. 9-17, 2005.

[25] H. T. L. F Xu, and Y. S. Wong, "Considerations and selection of optimal orientation for different rapid prototyping system," *rapid Prototyping Journal,* vol. vol. 5, pp. pp. 54-60, 1999.

[26] H. S. Ramanath, et al. , "Melt Flow Behaviour of Poly-Epsilon-Caprolactone in Fused Deposition Modelling," *Journal of Materials Science: Materials in Medicine* 2008.

[27] M. Roxas, "Fluid Dynamics Analysis of Desktop-based Fused Deposition Modeling Rapid Prototyping," University of Toronto,vol.1, pp.10-11 2008.

[28] http://curricula2.mit.edu/pivot/book/ph1301.html?acode=0x0200
.

[29] http://www.fjr1300.info/misc/torque-power.html.

[30] W. Michaeli, "Extrusion Dies for Plastics and Rubber: Design and Engineering Computation," vol. Second Edition, (1992).

[31] H. K. Versteeg and W. Malalasekera, *An introduction to computational fluid dynamics: the finite volume method*: Pearson Education, 2007.

[32] A. De Waele, "Viscometry and plastometry," *Oil Color Chem Assoc J*, vol. 6, pp. 33-88, 1923.

[33] W. Ostwald, "Ueber die geschwindigkeitsfunktion der viskosität disperser systeme. i," *Colloid & Polymer Science*, vol. 36, pp. 99-117, 1925.

[34] http://www.chem1.com/acad/webtext/dynamics/dynamics-3.html.

[35] S. G. E. Giap and M. Telipot, "The hidden property of Arrhenius-type relationship: viscosity as a function of temperature," *Journal of Physical Science*, vol. 2, pp. 29-39, 2010.

[36] S. Kalambur and S. S. Rizvi, "Rheological behavior of starch–polycaprolactone (PCL) nanocomposite melts synthesized by reactive extrusion," *Polymer Engineering & Science*, vol. 46, pp. 650-658, 2006.